Gondwana Research 39 (2016) 204–216

Contents lists available at ScienceDirect

Gondwana Research

journal homepage: www.elsevier.com/locate/gr

Density structure of the cratonic mantle in southern Africa: 1. Implications for dynamic topography

Irina M. Artemieva [a], Lev P. Vinnik [a,b]

[a] Geology Section, IGN, University of Copenhagen, Denmark
[b] Institute of Physics of the Earth, Moscow, Russia

ARTICLE INFO

Article history:
Received 26 July 2015
Received in revised form 21 February 2016
Accepted 3 March 2016
Available online 11 March 2016

Handling Editor: M. Santosh

Keywords:
Cratonic lithosphere
Mantle density
Dynamic topography
Upper mantle temperature
Kaapvaal and Zimbabwe cratons

ABSTRACT

The origin of high topography in southern Africa is enigmatic. By comparing topography in different cratons, we demonstrate that in southern Africa both the Archean and Proterozoic blocks have surface elevation 500–700 m higher than in any other craton worldwide, except for the Tanzanian Craton. An unusually high topography may be caused by a low density (high depletion) of the cratonic lithospheric mantle and/or by the dynamic support of the mantle with origin below the depth of isostatic compensation (assumed here to be at the lithosphere base). We use free-board constraints to examine the relative contributions of the both factors to surface topography in the cratons of southern Africa. Our analysis takes advantage of the SASE seismic experiment which provided high resolution regional models of the crustal thickness.

We calculate the model of density structure of the lithospheric mantle in southern Africa and show that it has an overall agreement with xenolith-based data for lithospheric terranes of different ages. Density of lithospheric mantle has significant short-wavelength variations in all tectonic blocks of southern Africa and has typical SPT values of ca. 3.37–3.41 g/cm^3 in the Cape Fold and Namaqua–Natal fold belts, ca. 3.34–3.35 g/cm^3 in the Proterozoic Okwa block and the Bushveld Intrusion Complex, ca. 3.34–3.37 g/cm^3 in the Limpopo Belt, and ca. 3.32–3.33 g/cm^3 in the Kaapvaal and southern Zimbabwe cratons.

The results indicate that 0.5–1.0 km of surface topography, with the most likely value of ca. 0.5 km, cannot be explained by the lithosphere structure within the petrologically permitted range of mantle densities and requires the dynamic (or static) contribution from the sublithospheric mantle. Given a low amplitude of regional free air gravity anomalies (ca. +20 mGal on average), we propose that mantle residual (dynamic) topography may be associated with the low-density region below the depth of isostatic compensation. A possible candidate is the low velocity layer between the lithospheric base and the mantle transition zone, where a temperature anomaly of 100–200 °C in a ca. 100–150 km thick layer may explain the observed reduction in Vs velocity and may produce ca. 0.5–1.0 km to the regional topographic uplift.

1. Introduction

The cratons of the southern Africa have an unusually high topography, 1.0–1.5 km on average, with an increase to 1.5–2.0 km in the eastern Kaapvaal and up to 2.5 km in Lesotho, and a depression down to 0.6–0.9 km in the Limpopo Belt (Fig. 1a). The topography of other cratons, including even the Archean parts of the Sino-Korean Craton which has been significantly affected by the India–Eurasia collision, is significantly lower, only 0.2–0.6 km (Fig. 2a, b). The only other high standing craton is the Tanzanian Craton, where the high topography may be caused by active mantle dynamics related to the Cenozoic rifting in East Africa. In southern Africa and the Tanzanian region, the high topography is a regional phenomenon that is observed both in the Archean and Proterozoic blocks, which have topography 500–700 m higher than any other craton worldwide (Table 1).

High surface elevation may result either from low density lithosphere or from the contribution (e.g. dynamic support) of the mantle below the LAB, or from the combination of both. The first factor is expected to play an important role in all Precambrian cratons, where the lithospheric mantle is depleted and has low-density (e.g. Gaul et al., 2000). In particular, petrological studies demonstrate that the lithospheric mantle beneath the Archean Kalahari Craton (which includes the Archean Kaapvaal and Zimbabwe cratons, melded along the Archean collisional Limpopo Belt) is depleted and has low-density (Boyd and Mertzman, 1987; O'Reilly and Griffin, 2006). Negative Bouguer anomalies (Fig. 3c) also indicate that low density material in the cratonic lithosphere contributes to high regional topography in southern Africa. Nonetheless, given a large number of craton-scale magmatic events in southern Africa (Fig. 1b), one may expect that the composition of the lithospheric mantle in the region could have been significantly modified through melt-metasomatism (Simon et al., 2007; Pearson and Wittig, 2008; Artemieva, 2009) with the

E-mail addresses: irina@ign.ku.dk (I.M. Artemieva), vinnik@ifz.ru (L.P. Vinnik).

http://dx.doi.org/10.1016/j.gr.2016.03.002
1342-937X/

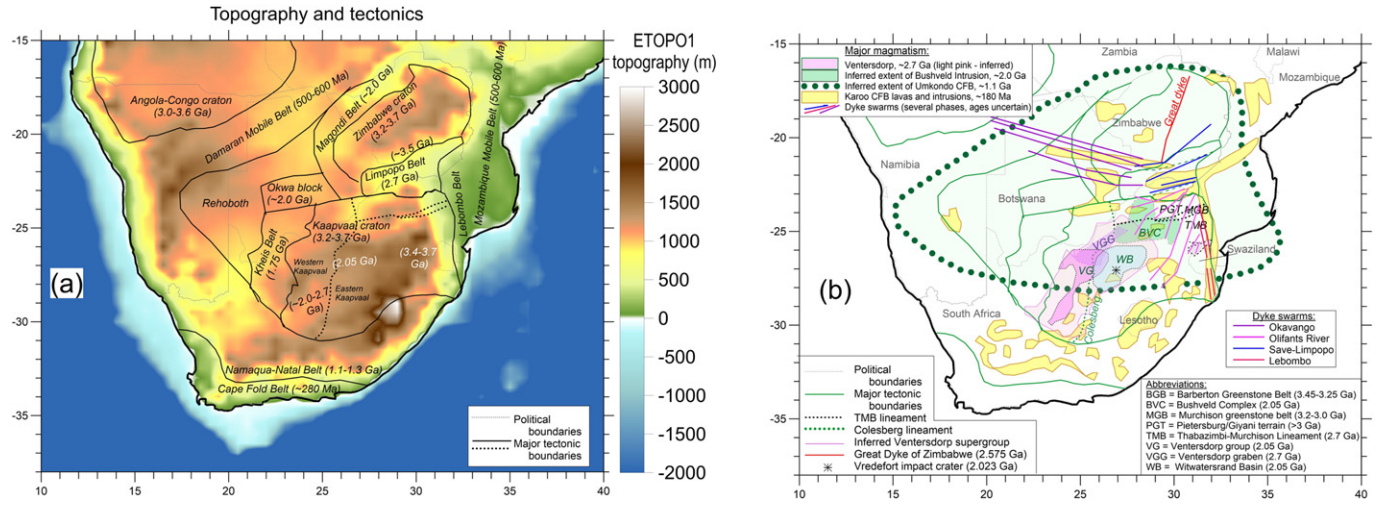

Fig. 1. Topography (a) (based on ETOPO1 global elevation model, Amante and Eakins, 2009) and major tectonic provinces (b) of the southern Africa. Tectonic boundaries — after de Wit et al. (1992) and Goodwin (1996); the Neoarchean Ventersdorp magmatic province — after Schmitz and Bowring (2003), the inferred extent of the Bushveld Igneous Complex — after Campbell et al. (1983) and of the Umkondo continental flood basalt province (CFB) — after Hanson et al. (2004); major Karoo lavas and outcrops — after Riley et al. (2006); locations and ages of kimberlites — based on database of Faure (2006).

corresponding increase in lithosphere mantle density, thus reducing the buoyancy contribution of the lithosphere to topography. Therefore, the dynamic support from the sublithospheric mantle (that is mantle residual topography caused by low density mantle anomalies of, primarily, thermal nature or dynamic topography caused by stresses associated with the mantle flow) should play an important role in providing high surface elevation in southern Africa. A simple comparison of topography in different cratons worldwide (Fig. 2a) suggests that the dynamic contribution of mantle convection to surface topography in the southern Africa is, at least, 500–700 m.

It has long been proposed that mantle plumes may have a strong effect on surface topography (Hager et al., 1985; Cox, 1989). Following this idea, the recent (Cenozoic) high topography of the southern Africa has been attributed to the dynamic effect of the proposed lower mantle plume (Lithgow-Bertelloni and Silver, 1998), which is seen as a ca. 1200 km wide, strong S-velocity anomaly (with a ca. 3% drop in Vs) in the lower mantle that extends upward from the core–mantle boundary to a depth of ca. 1500 km (Nyblade and Robinson, 1994; Ritsema et al., 1999; Ni and Helmberger, 2003). However, the wavelength of topographic uplift, if caused by the lower mantle plume, should be huge (comparable with large-scale geoid anomalies (Hager et al., 1985)) and significantly larger than the area with the high topography in southern Africa.

Despite an amazing number of publications on the African superplume and its effect on topography evolution (e.g. Hager et al., 1985; Gurnis et al., 2000; Simmons et al., 2007; Forte et al., 2010), there is still a lot of controversy in quantifying its dynamic effect because of a large uncertainty in mantle physical properties, particularly in mantle viscosity (Cadek and Fleitout, 2003). The values for dynamic topography in southern Africa range from near-zero (Forte et al., 2010) to more than 1.2 km (Flament et al., 2014); although many authors report the values around 600–700 m (Gurnis et al., 2000; Lithgow-Bertelloni and Silver, 1998; Conrad, 2013), which are consistent with our conclusion based on Fig. 2.

In a more general view, dynamic topography may be caused not only by temperature anomalies associated with mantle plumes, but by convective flow in the mantle which produces viscous stresses that may cause surface uplift above mantle upwellings (Hager et al., 1985) and basin subsidence above mantle downwellings (Heine et al., 2008; Downey and Gurnis, 2009). Numerical modeling of the dynamic effect

Table 1
Statistics for topography of Precambrian cratons worldwide.
Topography is derived from ETOPO1 global topographic model (Amante and Eakins, 2009) averaged on a 1° × 1° grid. Ages are based on the TC1 global lithosphere age model for the continents (Artemieva, 2006).

No. in Fig. 2	Region	All Precambrian		Archean only		Proterozoic only		[Archean topo] minus [Prot. topo], m
		Topo. average, m	St. dev., m	Topo. average, m	St. dev., m	Topo. average, m	St. dev., m	
1	Southern Africa cratons (south of 15S, excluding the Angola–Congo Craton)	1018	431	1053	369	983	472	70
2	Tanzanian craton (25–35N, 5N–10S)	952	390	948	389	958	398	−10
3	China cratons (east of 102E)	736	768	644	611	759	800	−115
4	West Africa, Congo, and Sahara (west of 25E, north of 15S)	531	345	623	371	471	280	152
5	Greenland	494	437	?		?		?
6	North America cratons	486	503	444	472	505	524	−61
7	Siberian Craton	474	416	635	405	323	247	312
8	South America cratons	338	408	413	302	325	418	88
9	India cratons	288	253	391	219	265	250	126
10	Australia cratons	278	177	302	164	268	184	34
11	East European Craton	178	150	160	86	185	165	−25
12	Arabia and Nubia shields (east of 30E, north of equator)	550	399	–		550	384	–

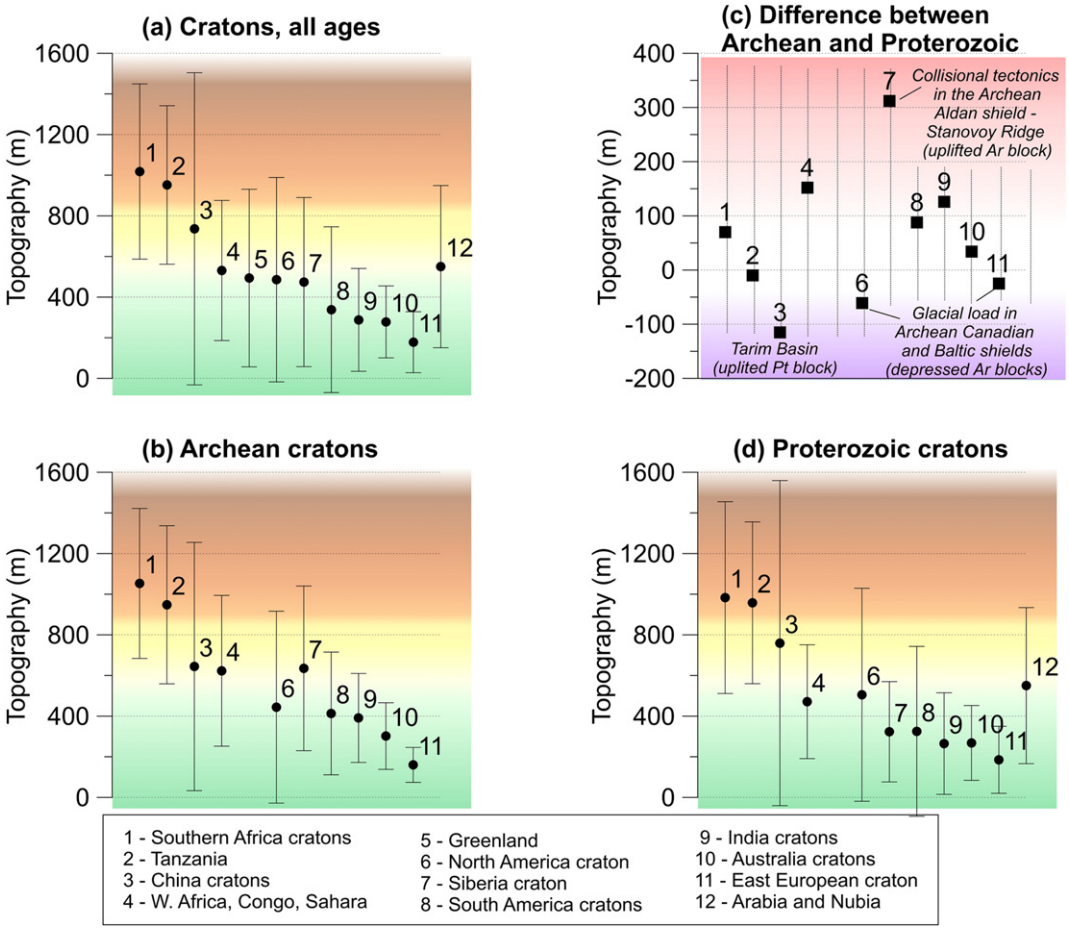

Fig. 2. Topography of different Precambrian cratons worldwide: (a) — all Precambrian terranes, (b) — only Archean blocks, (c) — difference between average topography of the Archean and Proterozoic blocks, and (d) — only Proterozoic blocks. Topography is derived from ETOPO1 global topographic model (Amante and Eakins, 2009) averaged on a 1° × 1° grid. Ages are based on the TC1 global lithosphere age model for the continents (Artemieva, 2006). Both Archean and Proterozoic blocks in the southern Africa and Tanzanian cratons are ca. 500–700 m higher than all other cratons worldwide. The high elevation of these two Precambrian regions may be attributed to a dynamic support from the sublithospheric mantle.

of mantle convection indicate that dynamic topography is characterized by small amplitudes (less than 300 m), long wavelengths (on order of ca. 1000 km), and slow rate of topographic changes (e.g. Braun, 2010). Studies of Neogene uplift in southern Africa indicate that it took place without stretching or shortening of the crust in two phases: with up to 0.3 km uplift at ca. 20 Ma and up to 0.9 km uplift during the last ca. 3 Ma (Artyushkov and Hofmann, 1998). These authors propose that regional uplift was caused by a rapid erosion of the lithosphere by a mantle plume. Similar values for the amplitude of vertical movements were reported in a recent analysis of sediments at the southwest African coastal shelf which suggest that ca. 0.5 km of topography is less than 5 Ma old, with an earlier phase of smaller uplift at ca. 30–35 Ma ago (Al-Hajri et al., 2009). Based on the amplitude of uplift (100–250 m/Ma) and the areal size of the topographic change (500–1000 km), these authors attribute the recent uplift of southern Africa to the dynamic effect of the lower mantle superplume. Other studies, however, suggest that, due to the relative northward motion of the African plate over the lower mantle superplume, its upwelling had a stronger impact on the East African Rift system rather than on the current high topography in southern Africa (Moucha and Forte, 2011). In such a case, it is the Tanzanian Craton where the high topography may be caused by mantle dynamics.

The concept of dynamic topography and the role of this mechanism in explaining high topography in various continental settings has recently been subject to a critical review (Molnar et al., 2015). These authors argue that free-air gravity anomalies are indicative of the role of mantle dynamics in supporting high terrains. Following the results by McKenzie (2010), they conclude that mantle flow (assuming an infinite depth of compensation) produces free air gravity anomalies of ca. 50 mGal for 1 km of topography. This rule of thumb would imply that, for free air anomalies of ca. 25 mGal typical of most of the southern Africa cratons (Fig. 3b), ca. 0.5 km of surface elevation may be supported by mantle flow (dynamic topography). However, if density anomalies in the mantle are located below the depth of isostatic compensation, they will not be seen in free air anomalies, while they may still contribute significantly to surface elevation. In this study, we demonstrate that this is likely to be the case in southern Africa.

In the present study we estimate a possible contribution of mantle dynamic and residual topography (associated either with viscous flow or with density anomalies in convective mantle) to the present high elevation of the southern Africa cratons from free-board constraints. The approach allows for separating the effect of isostatically compensated topography and the dynamic effect of the mantle on surface relief. We examine the contributions of the crust and the cratonic lithospheric mantle to the topography, and compare our estimates of the mantle density structure of the Kalahari craton with petrological data on xenolith-derived mantle peridotites and with regional seismic models of the lithosphere (Artemieva and Vinnik, in review). These independent data allow us to tighten constraints on the mantle (possibly dynamic) effect on the topography, and to examine the links between mantle density, seismic Vp, Vs in the mantle and the distribution of diamondiferous and non-diamondiferous kimberlites in southern Africa.

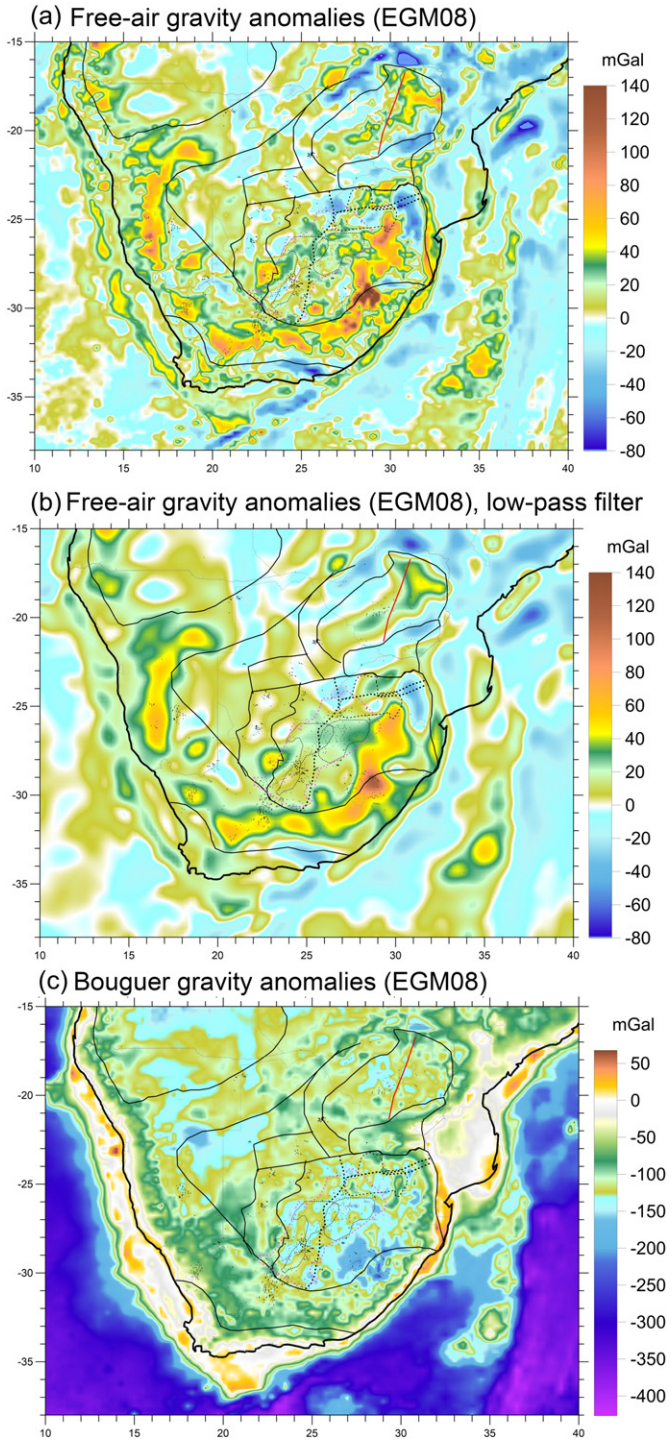

Fig. 3. Gravity anomalies in southern Africa. (a) Free air gravity anomalies (based on EGM08 gravity model, Pavlis et al., 2012), (b) free air anomalies with low pass filter; and (c) Bouguer gravity anomalies, calculated for crustal density of 2.67 g/cm^3 and water density of 1.03 g/cm^3.

2. Method

2.1. Data and model assumptions

The calculation approach is based on free-board modeling (Lachenbruch and Morgan, 1990), which we have applied earlier to examine density structure of the cratonic lithospheric mantle in the East European Craton (Artemieva, 2007) and Siberia (Cherepanova and Artemieva, 2015). For Siberia, the results of free-board modeling (Cherepanova and Artemieva, 2015) have been tested toward gravity modeling of mantle density anomalies (Herceg et al., 2015), and the results of the two independent approaches provide similar values of lithosphere mantle densities, which are also in good agreement with petrological data for mantle peridotites from the Siberian Craton.

The free-board approach assumes that the observed topography is the sum of crustal buoyancy, buoyancy of the lithospheric mantle, and dynamic topography. The latter is defined here as contribution from the mantle with the source deeper than the depth of isostatic compensation and it may be caused by viscous stress and/or density anomalies in convective mantle. The calculations are made on a 30 min × 30 min regular grid, and all model parameters are interpolated to this grid. The approach is based on the following assumptions:

- The region is in isostatic equilibrium; this assumption is justified by small free air gravity anomalies typical for most of the Kalahari Craton, except for Lesotho where free air anomalies reach ca. +100 + 200 mGal (Fig. 3a); the isostatic balance is assumed to be achieved at the base of the lithosphere (the LAB);
- Flexural rigidity of the lithosphere is ignored, suggesting that the individual lithospheric blocks can move independently as piano keys. Although this assumption is not directly supported by the available estimates of effective elastic thickness (72 km for the Archean Kaapvaal Craton and 38–48 km for the Mesoproterozoic Namaqua–Natal Mobile Belt) (Doucoure et al., 1996), the latter results indicate that the Kaapvaal Craton and the Namaqua–Natal Belt are mechanically decoupled and behave as separate domains. We will demonstrate later that this conclusion is consistent with our results;
- The topography (based on ETOPO1 global elevation model (Amante and Eakins, 2009)) is the sum of the lithosphere buoyancy and the unknown dynamic topography produced by viscous stress and/or density anomalies in convective mantle;
- As in classical isostasy, the crustal and mantle buoyancies are controlled (i) by the thicknesses of, correspondingly, the crust and the lithospheric mantle and (ii) by the density contrast between the asthenosphere and, correspondingly, the crust and the lithospheric mantle;
- The Moho depth is constrained by the receiver function (RF) analysis of the SASE (the Southern African Seismic Experiment) data with regionally variable Vp/Vs ratio (Youssof et al., 2013) (Fig. S1). Although the RF analysis indicates the presence of strong compositional heterogeneity in the crust of southern Africa (Youssof et al., 2013), we adopt the constant value of 2.85 g/cm^3 as average crustal density at SPT conditions, given the non-uniqueness of Vp/Vs conversion to density (Fig. S2);
- Density of the lithospheric mantle is the second unknown in the calculation set-up (in addition to dynamic topography) and it is determined by subtracting the calculated crustal buoyancy and the assumed dynamic topography from the observed topography (see details below);
- Density of the sublithospheric mantle (asthenosphere) is assumed to be constant and equals to 3.39 g/cm^3 at SPT conditions (Irifune, 1987) or 3.235 g/cm^3 at in situ conditions (at T = 1300 oC and assuming thermal expansion coefficient of 3.5×10^{-5} 1/K);
- The base of the lithosphere is defined by a 1300 °C isotherm (Fig. 4b) and we assume steady-state thermal conduction within the lithosphere which allows for calculating lithosphere geotherms from surface heat flow (Fig. 4a) (Artemieva and Mooney, 2001). The average temperature of the lithospheric mantle is defined as mid-temperature between temperature at the Moho (locally variable depending on regional geotherms) and at the lithosphere base;
- We ignore the pressure-dependence of density, but account for thermal expansion and the corresponding variations in crustal and lithosphere mantle densities;

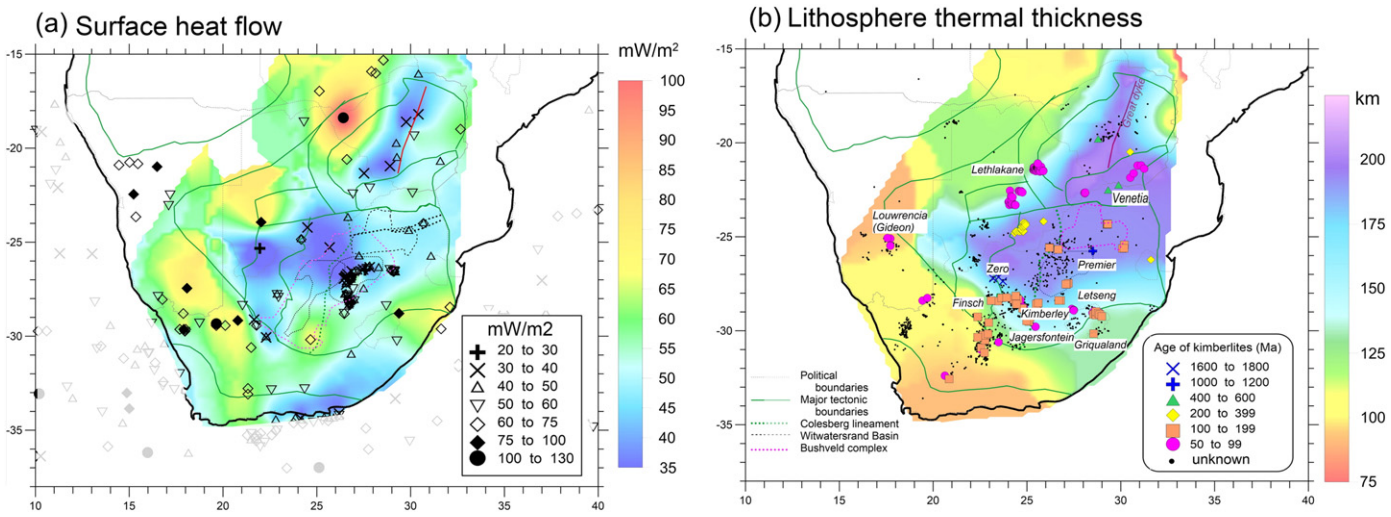

Fig. 4. Lithosphere thermal state in southern Africa. (a) Surface heat flow (based on IHFC database, IHFC, 2011), and (b) lithosphere thermal thickness constrained by heat flow data (Artemieva and Mooney, 2001). Locations and ages of kimberlites — based on global compilation (Faure, 2006).

- The free-board approach includes a free parameter which is topography at mid-ocean ridge. We adopt the value of 4.25 km which is based on the analysis of the segment of mid-ocean ridge (SE Pacific ocean) with zero free air gravity anomaly (local isostatic compensation) and available seismic data on the crustal structure (Cherepanova and Artemieva, 2015).

2.2. Calculation procedure

As mentioned above, the calculation scheme includes two unknown parameters: (i) the dynamic contribution to the topography from the mantle and (ii) the density structure of the lithospheric mantle, which we both want to determine. This requires additional assumptions. Given that dynamic topography is expected to be caused by convective flow in the mantle or by mantle density/temperature anomalies, we expect that it should have a long wavelength (at least 500–1000 km) and contribute ca. 0.5–0.7 km to the surface topography (as Fig. 2 implies). Density variations in the lithospheric mantle may have a short wavelength, and they may additionally contribute locally to the high topography in southern Africa.

We split the analysis into two parts. We first examine the possible range of dynamic topography values by assuming a constant density of the lithospheric mantle for the entire region and compare them with our preliminary conclusions based on Fig. 2. We next calculate the density structure of the lithospheric mantle for several values of dynamic topography and compare the results with petrological data on mantle density.

2.2.1. Step 1

To resolve the competing effects of dynamic topography and buoyancy (density) of the lithospheric mantle, we first assume the constant density of the lithospheric mantle for the entire region and adopt the value of 3.38 g/cm^3 as typical of the Phanerozoic, and possibly the Proterozoic, mantle (Gaul et al., 2000), which is widespread along the southern margin of the Kaapvaal Craton (Fig. 1a). Under this assumption and for the realistic choice of other model parameters such as average crustal density and density of sublithospheric mantle (discussed further in the uncertainty analysis, Figs. 5, 6 and S4), the dynamic topography in the Cape Fold Belt and the Namaqua–Natal Belt (Fig. S3) is ca. 0.5–1.0 km, similar to what Fig. 2 suggests.

We note that by the calculated value of dynamic topography and in agreement with studies of effective elastic lithosphere (Doucoure et al., 1996), the region splits into two coherent blocks: one of them includes the Archean Kaapvaal–Zimbabwe cratons, and the other — the late Proterozoic Namaqua–Natal and the Phanerozoic Cape Fold belts (ca. 280 Ma) (the pattern is particularly well seen in Fig. S3a, b, c). The presence of two coherent blocks in the lithosphere structure of the region justifies our assumption that, at first order, flexural rigidity may be ignored in the analysis of the dynamic and buoyancy effects on the southern Africa topography.

We, however, assume that if the source of dynamic topography is below the depth of isostatic compensation, its value should be closely the same for the entire region. The analysis of models with different choice of parameters shows that models with high crustal density (Fig. S3a) and thick lithosphere (Fig. S3c) require very high dynamic contribution to topography (>3 km). These models are unrealistic, because they would require unrealistically low mantle density in the Archean blocks (outside the petrologically defined range, Fig. 7) in order to reduce dynamic topography to values <1 km in agreement with Fig. 2. The model with moderately depleted mantle (3.35 g/cm^3) requires negative values of dynamic topography for the Proterozoic blocks and parts of the Limpopo Belt (Fig. S3d), but reduces the value of dynamic topography in the Archean blocks to ca. 0.5–1.5 km. Because of the negative values of dynamic topography for significant parts of the craton, we reject this model, although it clearly demonstrates that low density lithosphere mantle in the Archean blocks is required by data. The model with an average crustal density of 2.85 g/cm^3 and a lithosphere mantle density fixed at 3.38 g/cm^3 for the entire region (Fig. S3b) requires ca. 0.5 km of dynamic support for the Proterozoic blocks and ca. 1.0–1.5 km of unexplained topography for the Archean blocks. The latter can be also reduced to ca. 0.5 km of dynamic support for petrologically permitted range of lithosphere mantle density (Figs. 7, 8a, b c, see below).

2.2.2. Step 2

Based on the preliminary analysis (Figs. 2 and S3), we next adopt the values of 0.5 km and 1.0 km for the dynamic topography for calculating the density structure of the lithospheric mantle (Figs. 8, 9). We also calculate the results for least realistic cases when dynamic topography is set zero and 2 km (Figs. S5 and S6). The assumption on a 2 km contribution of dynamic topography to surface relief leads to unrealistically high mantle density in significant parts of the region (Fig. S6). Importantly, if dynamic topography is assumed to be zero (Fig. S5),

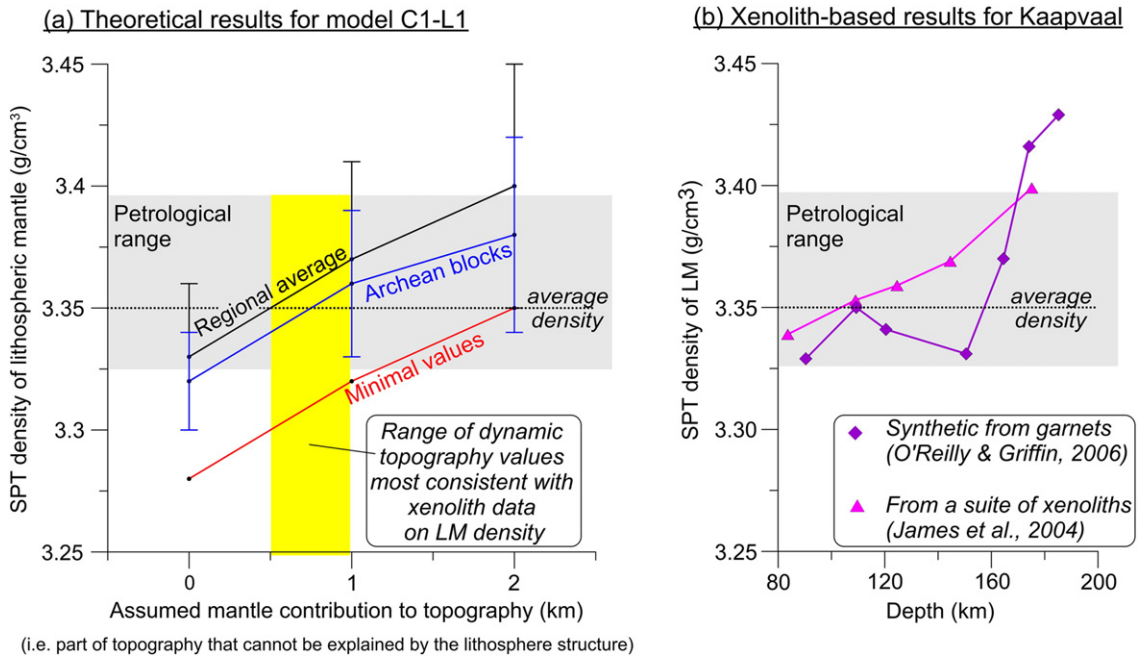

Fig. 5. Uncertainty analysis for the possible parameter space: (a) predicted density of the lithospheric mantle as function of the assumed value of dynamic topography (for model with crustal density of 2.85 g/cm^3); black line — regional average; blue line — average for the Archean blocks; red line — minimal regional values; gray shading — range of lithospheric mantle density consistent with xenolith data; yellow shading — range of dynamic topography values which provides the best match between the predicted values of lithospheric mantle density and regional petrological data (b). Petrologic models (b) are SPT density of the Kaapvaal lithospheric mantle as a function of age calculated from garnets (O'Reilly and Griffin, 2006) and from a suite of xenoliths (James et al., 2004) from group I Kaapvaal xenoliths. For both data sets average density is 3.366 g/cm^3 for the depth range 80–200 km and ca. 3.35 g/cm^3 for the depth range 80–170 km (dotted line).

the estimated values of lithosphere mantle density are significantly lower than the values based on petrological studies of mantle-derived xenoliths from southern Africa. We therefore conclude that it is impossible to fit the lithosphere mantle density to the petrologically permitted range (Fig. 7) if dynamic topography is assumed to be zero.

2.3. Sensitivity analysis

The results of the sensitivity analysis are illustrated in Fig. S3 and are summarized in Figs. 5, 6. By varying major (and most uncertain) model parameters (average crustal density, density of the lithospheric mantle,

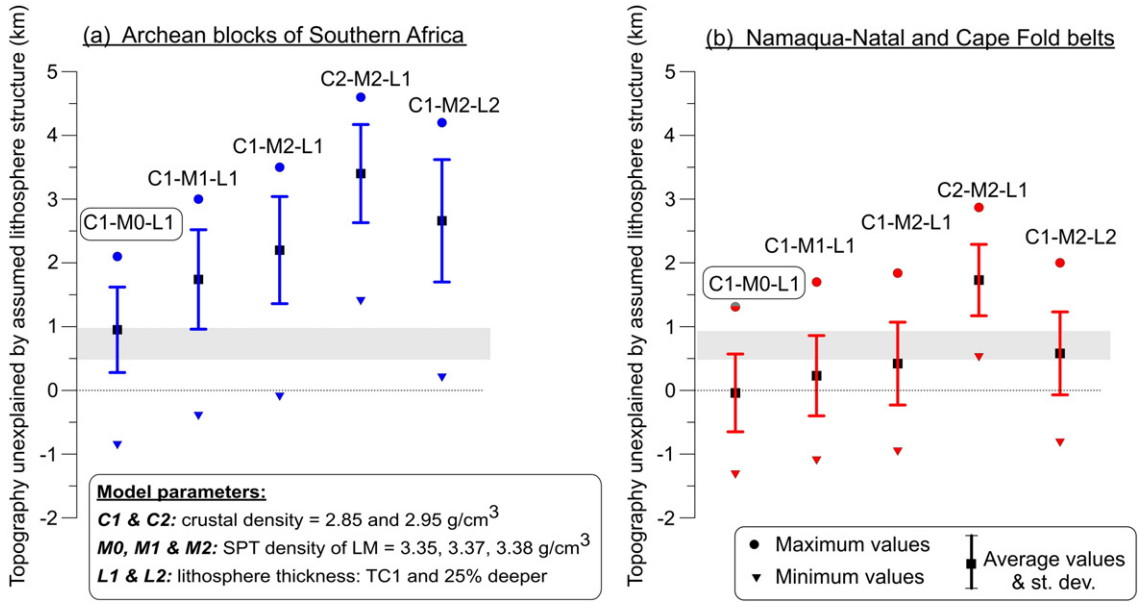

Fig. 6. Predicted values of dynamic topography for the Archean (a) and Proterozoic–Phanerozoic blocks (b) calculated for five test models with different lithosphere parameters (Fig. S3). The results are calculated on a 30 min × 30 min grid; minimum and maximum values show the span of values for the entire region; vertical bars show the average for the entire region and standard deviation for each of the models. Models which require the smallest values of dynamic support from the sublithospheric mantle have average crustal density of 2.85 g/cm^3 and lithosphere thickness of ca. 200 km in the Archean blocks (Fig. 4b). There are only two models (C1-M0-L1 and C1-M1-L1) which require a similar mantle contribution to topography (between 0.5 and 1.0 km) for both the Archean (a) and Proterozoic–Phanerozoic (b) blocks. Gray shading — extra regional topography as indicated in Fig. 2.

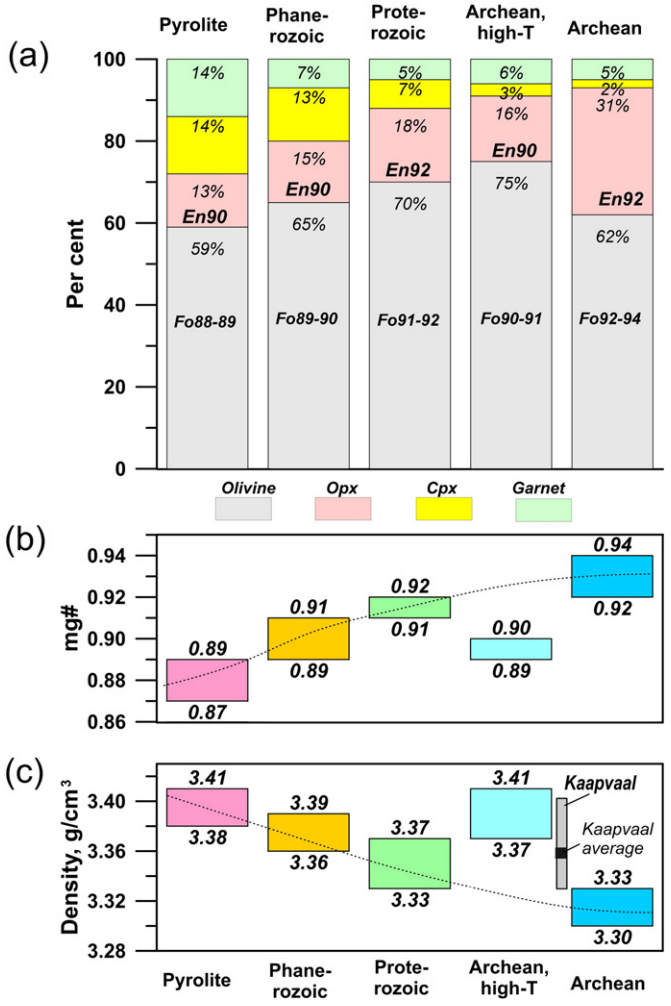

Fig. 7. (a) Average model composition of the continental lithospheric mantle and mantle pyrolite (asthenosphere) (based on data of Griffin et al., 1998). (b–c) Secular trends in average olivine mg# = Mg/[Mg + Fe] and density (at SPT conditions) of the lithospheric mantle calculated from average mineral compositions of garnet peridotites (data of Hawkesworth et al., 1990; Griffin et al., 1998, 1999). The ranges of global and regional values are shown for both parameters. Gray insert in (c) — the range of density values typical of the Kaapvaal lithosphere mantle.

lithosphere thickness and the corresponding geotherms) we analyze the sensitivity of the results to the choice of the model parameters. The following sets of parameters are analyzed (labels in brackets correspond to the labels in Figs. 5, 6):

- average crustal density of 2.85 g/cm^3 (C1) and 2.95 g/cm^3 (C2); the latter value requires the presence of a thick high-velocity lower crustal layer;
- density of the lithospheric mantle used at step 1 (calculation of dynamic topography) 3.35 g/cm^3 (M0), 3.37 g/cm^3 (M1) and 3.38 g/cm^3 (M2) at SPT conditions; the latter density value corresponds to fertile composition which may be expected only in the southern parts of the region, outside of the Archean blocks;
- lithosphere thickness as determined from heat flow (Artemieva and Mooney, 2001) (L1) and 25% thicker (L2), with the corresponding adjustment of lithospheric geotherms.

We do not present tests for smaller values of the lithosphere thickness, although a number of seismic estimates of thickness of the lithosphere suggest that it can be 160–200 km thick. Most published estimates of depth of the seismic LAB in southern Africa are obtained from inversion of dispersion curves of Rayleigh waves, where the LAB at 160–200 km depth is defined as the top of the low S-wave velocity layer (e.g. Priestley et al., 2006; Li and Burke, 2006). S-wave velocity in such models will vary slowly with depth even if the lithosphere–asthenosphere boundary is sharp, and therefore the depth of the LAB cannot be determined precisely. Another approach to estimating the depth of the LAB by seismic means is based on the analysis of azimuthal anisotropy. In such definition, the LAB corresponds to the transition from frozen to active seismic anisotropy, and the depth of this transition can be evaluated accurately from receiver functions. The depth thus obtained is 160 km in southern Africa (Vinnik et al., 2012). The presence of the rheological boundary at a ca. 140–160 km depth within the Kaapvaal lithosphere is also supported by grain size variations (Mercier, 1980). This depth also corresponds to the transition from depleted to fertile mantle (Fig. 5b) as reported in a number of petrological studies (e.g. O'Reilly and Griffin, 2006), and similar observations were reported for the Slave Craton and the Central Finland province of the Baltic shield (Kopylova and Russell, 2000; Lehtonen et al., 2004). However, xenolith data indicates that in all of these cratons the lithosphere extends deeper than 160 km depth, and to ca. 180–250 km in Kaapvaal (e.g. Rudnick and Nyblade, 1999; Griffin et al., 2003).

In the case of thick lithosphere (L2) or heavy crust (C2), the values of dynamic topography become unrealistically high (compare Fig. S3b with Fig. S3ac), ca. 1–2 km for the Namaqua–Natal Belt and ca. 2.5–3 km for the Archean blocks (Fig. 6). These high values of dynamic topography cannot be reduced to 0.5–1.0 km by replacing the assumed density of the lithospheric mantle (3.38 g/cm^3) by low-density values within the range reported by petrological studies of mantle xenoliths. We thus reject models L2 and C2 from further consideration.

Models with a slightly different density of the lithospheric mantle (3.38 and 3.37 g/cm^3 at SPT conditions) produce similar values of dynamic topography south of the cratonic margin (0.5–1.0 km), which are consistent with the expectations based on global analysis of topography in the cratons (Fig. 2) and numerical modeling (Lithgow-Bertelloni and Silver, 1998). We further use both of these models (parameterized with C1 and L1, for dynamic topography of 0.5 and 1.0 km) towards calculations of mantle density anomalies for the entire southern Africa along the SASE seismic stations (Figs. 8, 9). To check if these models provide realistic results, we calculated the density of the lithospheric mantle (at SPT condition) for lithosphere models parameterized with C1-L1 values and assuming different values of dynamic topography (Fig. 5a). The C1-L1 model provides good fit to regional petrological data for Kaapvaal (Fig. 5b) when dynamic topography is between ca. 0.5 and 1.0 km.

Due to a significant uncertainty in the model parameters, we also examine the results for any possible systematic trends (Fig. S4). Our special focus is on crustal density and we examine correlation between the calculated mantle density and the crustal Vp/Vs ratio as determined from RF interpretations of the SASE seismic data (Youssof et al., 2013). Lack of correlation suggests that there are no systematic links between the composition of the crust (as reflected in Vp/Vs ratio) and the density anomalies within the lithospheric mantle, and thus our assumption on the constant crustal density does not introduce any systematic bias into the final results (although it certainly produces some errors which cannot be assessed due to the non-uniqueness of Vp/Vs conversion to density (Fig. S2) and the absence of direct information on the crustal density structure).

We find that some correlation exists between the calculated mantle density and thickness of the crust (Fig. S4b). Given that most of the region is close to isostatic compensation (Fig. 3a), we find it likely that there can be a true correlation between the structure of the crust and the lithospheric mantle: regions with a deep Moho commonly (even in the cratonic settings) have a layer of underplated material in the lower crust (Thybo and Artemieva, 2013). The presence of underplated material indicates magmatic additions to the lithosphere, which are

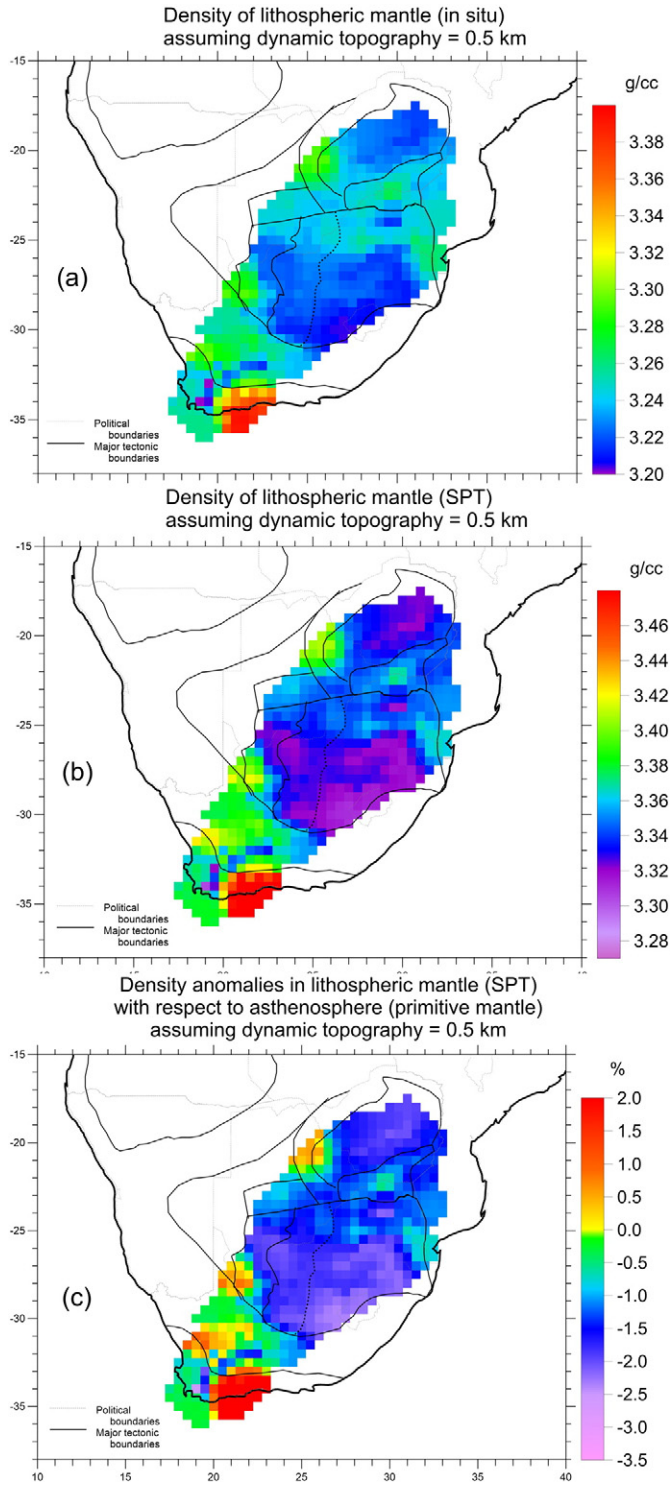

Fig. 8. Density of lithospheric mantle at in situ (a) and SPT (b) conditions at Earth's surface, and as density anomaly (c) with respect to convective mantle with density of 3.39 g/cm^3 (at SPT conditions). The maps are calculated assuming dynamic or residual mantle contribution to topography is 0.5 km. The estimated values of lithosphere mantle density are within the range of values based on petrological studies of mantle-derived xenoliths from southern Africa and worldwide (Fig. 7). Very high density anomaly in the Eastern Cape Fold belt is probably an artifact which propagates from the crustal model (Fig. S1). For interpolated version of (c) see Graphical Abstract.

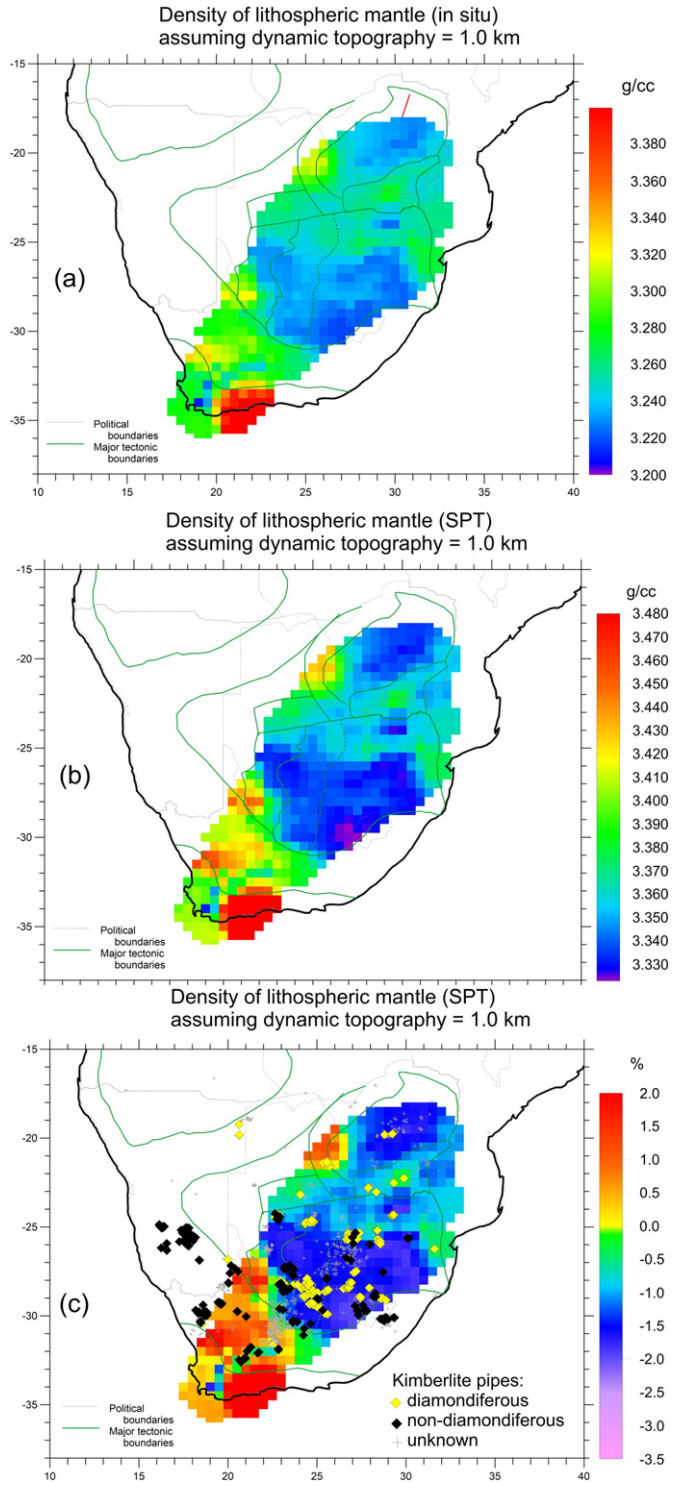

Fig. 9. Density of lithospheric mantle at in situ (a) and SPT (b) conditions, and as density anomaly (c) with respect to convective mantle with density of 3.39 g/cm^3 (at SPT conditions). The maps are calculated assuming dynamic or residual mantle contribution to topography is 1.0 km. The estimated values of lithosphere mantle density are within the range of values based on petrological studies of mantle-derived xenoliths from southern Africa and worldwide (Fig. 7). Distribution of diamondiferous and non-diamondiferous kimberlites is shown in (c). All diamondiferous pipes are restricted to the lithospheric mantle with low density (high depletion). Very high density anomaly in the Eastern Cape Fold belt is probably an artifact which propagates from the crustal model (Fig. S1).

expected to produce melt-metasomatism in the cratonic lithospheric mantle, with the corresponding increase in its density (e.g. Griffin et al., 2005). We therefore consider the trend in Fig. S4b as real and probably reflecting paleocollision-related magmatism.

We also observe a weak correlation between in situ density anomalies in the lithospheric mantle and lithosphere thickness (Fig. S4d). Regions with low density mantle tend to have thicker lithosphere.

This correlation reflects the age-dependent global patterns in mantle density structure (Fig. 7) and lithosphere thickness.

3. Density structure of the lithospheric mantle

Under the assumption that dynamic topography produces either 0.5 km or 1.0 km of surface elevation in southern Africa, we calculate density variations in the lithosphere mantle. Our approach provides only the depth averaged values of density, and the depth distribution of possible density anomalies within the lithosphere mantle cannot be resolved. We present the results for:

- in situ density of the lithospheric mantle (which allows direct comparison with seismic models and with mantle gravity anomalies),
- SPT (P–T conditions at the Earth's surface) density of the lithospheric mantle (which allows direct comparison with petrological data),
- density anomaly with respect to fertile mantle (which provides measure on the degree of mantle depletion).

The results show strong heterogeneity of the density structure of the lithospheric mantle, where regional variations are strongly correlated with surface tectonics. We next discuss the major features from south to north, with focus on the results calculated for a 0.5 km contribution from dynamic topography, which we assume to be the most realistic case (Fig. 8). The modeling results for other assumed values of dynamic topography are shown in Figs. 9, S5, S6. The difference between two models with realistic values of dynamic topography (1 km and 0.5 km) is shown in Fig. S7. Further discussion of mantle density structure for different tectonic provinces of southern Africa is presented in the companion paper (Artemieva and Vinnik, in review), where the links between the mantle density structure, mantle velocity structure and kimberlite magmatism are examined as well.

3.1. Cape Fold Belt (ca. 280 Ma)

Geologically, the Cape Fold Belt is made of two provinces, Western and Eastern. The Western province includes late Precambrian Cape granites which intruded the Precambrian (1.2–0.5 Ga) basement during the Saldanian Orogeny (a part of the Pan-African orogenic belt Belt formed during the convergence of South American and Namibian cratons (Rozendaal et al., 1999)). The results demonstrate that the Western Cape Fold Belt has moderately depleted lithospheric mantle with SPT density of 3.37 g/cm^3 (which corresponds to density deficit of −0.5% with respect to the primitive mantle and is within the range expected for the Phanerozoic mantle, Fig. 7c). Some blocks (with high topography and low mantle density of 3.33 g/cm^3) apparently may have extremely high mantle depletion, similar to the Kaapvaal Craton (Fig. 8).

The Eastern Cape Fold Belt has a high density mantle, with a sharp boundary in mantle density between the Western and the Eastern blocks. However, the mantle densities calculated for the Eastern Cape Fold Belt are unrealistically high (3.46–3.50 g/cm^3) and could be explained by the presence of a significant amount of eclogite in the mantle, such as associated with subducted oceanic slabs. Nonetheless, we consider these high values as an artifact result of strong anomalies in the Moho depth (Fig. S1) and in Vp/Vs ratio (1.6) calculated for this region (Youssof et al., 2013). These very high mantle density values also suggest that the average crustal density in this block may be significantly higher than the assumed value of 2.85 g/cm^3. The presence of underplated very high-density material within the lower crust of the collisional orogen is possible (e.g. as observed in the Urals, Kashubin et al., 2006), but no definitive conclusions may be made in the absence of high-resolution seismic refraction studies in the Eastern Cape Fold Belt.

3.2. Namaqua–Natal Belt (1.1–1.3 Ga)

The Namaqua–Natal Belt has a highly heterogeneous structure of the lithosphere mantle density. Overall, the calculated values are typical of fertile mantle (3.37–3.41 g/cm^3 at SPT conditions, Fig. 7). The central part of the Namaqua–Natal Belt is crossed by a narrow belt of depleted mantle (SPT density 3.34–3.36 g/cm^3) tending roughly in the SW–NE direction (Figs. 8b, 9b). We note that most kimberlite pipes within the Namaqua–Natal Belt follow this belt of depleted lithosphere. The results suggest that the western part of the area may have a fertile mantle (3.40–3.41 g/cm^3).

3.3. Kheis Belt and Okwa block (1.7–2.0 Ga)

By mantle density structure, the Kheis Belt splits into two parts. The southern part which has been affected by the Eburnean orogeny (ca. 2.0 Ga) may have fertile mantle, with density of ca. 3.37–3.41 g/cm^3. The northern part of the Kheis Belt has a highly depleted, low-density lithospheric mantle, similar to the Kaapvaal Craton. The strongest density deficit (−2.5% with respect to primitive mantle) is in the central part of the Kheis Belt. The lithosphere mantle of the Okwa block is depleted and has density of 3.35–3.36 g/cm^3. According to petrological studies of xenolith-derived xenoliths, such values are typical of the Proterozoic mantle worldwide (Gaul et al., 2000).

3.4. Kaapvaal Craton (3.2–3.7 Ga)

Along the southern rim of the craton, the transition from the fertile mantle of the Namaqua–Natal Belt to the highly depleted mantle of the Kaapvaal Craton nearly corresponds to geological boundaries. We note only a very weak difference in mantle density between the western and eastern blocks of Kaapvaal (3.32–3.34 g/cm^3 for the western block versus 3.31–3.33 for the eastern block), although the eastern block appears to be slightly more depleted. An increased mantle density marks the Witwatersrand Basin (2.05 Ga) of the eastern block.

The results for Lesotho (SPT density of 3.31 g/cm^3) should be considered with caution since this region of extremely high topography (2.5 km) has free air anomalies of +100 + 150 mGal and is not isostatically compensated (Fig. 3a). Similarly, a very low density mantle to the north-east from Lesotho is calculated for the region where free air gravity anomalies are ca. +100 mGal.

Surprisingly, relatively high mantle density (3.35–3.36 g/cm^3) atypical of the normal Archean mantle is characteristic of the ancient terrains around the Barberton greenstone belt (Fig. 11). We note that this region is also not fully isostatically compensated (free air anomaly is ca. −50 − 60 mGal).

The ca. 2.05 Ga Bushveld Intrusion Complex in the northern part of the Kaapvaal Craton is clearly marked by an increased density of the mantle (3.34–3.35 g/cm^3), typical of the Proterozoic rather than the Archean mantle (Fig. 10c). The pattern is particularly evident in Fig. 9b, c. In agreement with earlier petrological studies, we attribute increased mantle density to melt-metasomatism associated with the emplacement of this igneous complex (Carlson et al., 1999; Irvine et al., 2001). From the pattern of mantle density anomalies, the Bushveld complex appears as a coherent structure in the lithospheric mantle with no difference between the western and the eastern lobes. This result, which is best seen for the case of 1.0 km dynamic topography (Fig. 9), supports the same conclusion based on the analysis of the regional crustal structure (Youssof et al., 2013). A small block of undisturbed Kaapvaal mantle with low density (3.32–3.33 g/cm^3) has been preserved between the eastern lobe of the Bushveld complex and the Limpopo Belt (the Pietersburg/Giyani terrain, Fig. 1b).

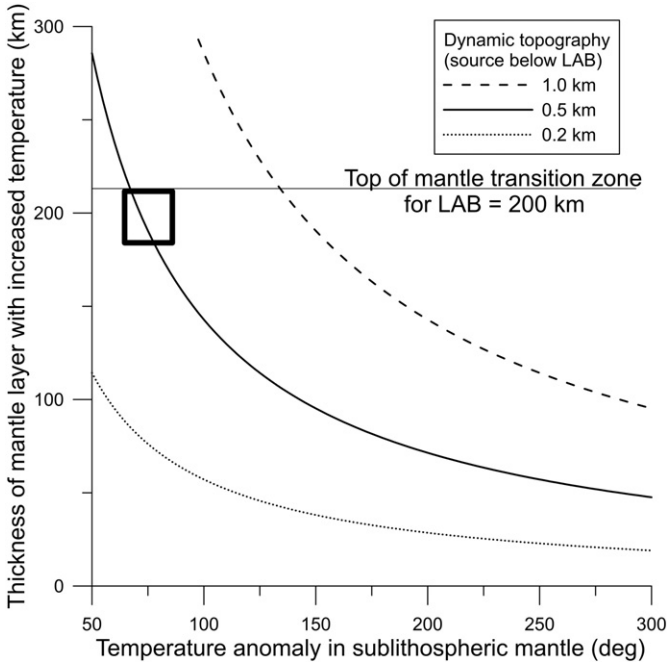

Fig. 10. Thickness of the upper mantle layer (below LAB) with an increased temperature versus temperature anomaly. Temperature and density anomalies in the upper mantle below the LAB which can provide mantle (dynamic) contribution to surface topography of 0.2 km, 0.5 km, and 1.0 km. A 0.5 km of surface uplift may be caused by a 75 oC temperature anomaly in a 200-km thick layer between the LAB and the top of the transition zone, or by a 150 . oC temperature anomaly in a 100-km thick layer.

3.5. Limpopo Belt (2.7–3.0 Ga)

Together with the Bushveld complex, the Limpopo Belt separates two depleted cratonic nuclei of the Kaapvaal and Zimbabwe cratons. This belt, which contains a set of paleo-subduction systems, represents a significantly reworked Archean mantle (peridotite xenoliths from the Venetia kimberlite pipe in central Limpopo Belt (see Fig. 4b for location) have Archean Re-depletion ages of ca. 3.0 Ga, Carlson et al., 1999). The Limpopo Belt is clearly expressed by increased mantle density (3.34–3.37 g/cm^3) typical of metasomatised cratonic roots.

The least depleted mantle of the Limpopo Belt is beneath its central part (Fig. 8) and it is sampled by the Cambrian diamondiferous Venetia and River Ranch kimberlites. Petrological studies suggest that the bottom portion of the lithospheric mantle beneath these two pipes may represent a southward continuation of the depleted Tokwe block of the Zimbabwe Craton (Smith et al., 2009). Our results, which cannot constrain the depth distribution of density anomalies, do not rule out this possibility. Intermediate bulk density of the Limpopo lithospheric mantle may be a result of vertical averaging of a depleted mantle at the base of the lithospheric mantle and a fertile mantle in its upper section (or vice versa, as suggested by xenoliths studies for a number of Archean terranes (Kopylova and Russell, 2000; Lehtonen et al., 2004).

Given that the eastern Limpopo Belt was the locus of several giant dyke swarms, it is surprising that the western and eastern parts of the belt have a similar bulk density structure of the lithospheric mantle. A possible explanation is that the crustal density structure is significantly different in the eastern and western parts of the Limpopo Belt. We discuss the links between the mantle density structure and kimberlite magmatism in the companion paper (Artemieva and Vinnik, in review).

3.6. Zimbabwe Craton (2.8–3.7 Ga)

The mantle density in most of the Zimbabwe Craton, including the eastern Tokwe block, is similar to the Kaapvaal Craton (3.32–3.33 g/cm^3 at SPT conditions, which corresponds to −1.5–2% of density deficit). However, in the western part (2.6–2.8 Ga) of the craton mantle is fertile and its density increases from 3.37 g/cm^3 to 3.40 g/cm^3 toward the Magondi Belt. The Great Dyke of Zimbabwe crosses the most depleted part of the craton and it is not seen in mantle density structure, supporting the geological evidence that this is a shallow crustal feature.

4. Upper mantle origin of dynamic topography

Our results for the density structure of the lithospheric mantle based on the assumption of a 0.5–1.0 km dynamic topography agree with regional petrological data. The value of dynamic topography of 0.5–0.7 m is also supported by the comparison of topography between different cratons worldwide (Fig. 2). We therefore conclude that 0.5–1.0 km of topography, with the most likely value of ca. 0.5 km, cannot be explained by the lithosphere structure and requires the contribution from the sublithospheric mantle, such as a dynamic support associated with mantle flow, or a static support by a low-density anomaly. Because free air gravity anomalies are small in most of the region (ca. +20 mGal on average), we propose that extratopography is related to the mantle structure below the depth of isostatic compensation (the LAB). Given that the wavelength of high topography in southern Africa is small (less than 1000 km) and its age is younger than ca. 30–35 Ma (Artyushkov and Hofmann, 1998; Al-Hajri et al., 2009), the origin of dynamic topography is unlikely to be related to the lower mantle superplume.

A surface uplift of 0.5 km may be caused by a 75 °C temperature anomaly in a 200-km thick layer between the LAB and the top of the transition zone, or by a 150 °C temperature anomaly in a 100-km thick layer (Fig. 10). A temperature anomaly of 75 °C will produce velocity anomalies of ca. 0.5% for Vp and ca. 1% for Vs, and double Vp, Vs anomaly values in case of a 150 °C anomaly (Cammarano et al., 2003). Velocity anomalies less than 1% may be not reliably resolved by seismic tomography (Foulger et al., 2013). However, Vs anomalies of around −2%–3% are in the range of those found in the sublithospheric mantle beneath the Kalahari Craton (Fig. 11, e.g. Wang et al., 2008). We next examine several possibilities for depth extent of the upper mantle layer responsible for regional dynamic topographic uplift.

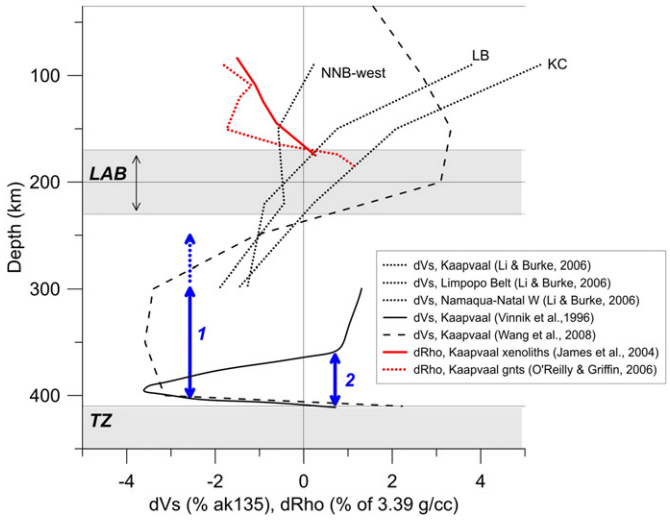

Fig. 11. Seismic Vs anomalies (shown with respect to ak135 model) in the upper mantle of southern Africa (Vinnik et al., 1996; Li and Burke, 2006; Wang et al., 2008). Red lines — density anomalies calculated from garnets (O'Reilly and Griffin, 2006) and from a suite of xenoliths (James et al., 2004) from Group I Kaapvaal xenoliths. Gray shadings — lithosphere-asthenosphere transition (LAB) and mantle transition zone (TZ). Blue arrows mark the depth regions with low seismic Vs between the LAB and TZ; these upper mantle layers may be responsible for ca. 0.5–1.0 km of dynamic topography (see text for discussion). Abbreviations: KC = Kaapvaal Craton, LB = Limpopo Belt; NNB = Namaqua–Natal Belt.

Seismic studies of the mantle beneath the Kalahari Craton, especially those based on the observations of Rayleigh wave dispersion, provide evidence of S velocity reduction of ca. 4% relative to the overlaying high-velocity lid in a depth range from ~150 to ~250 km (Priestley et al., 2006). The results of joint inversion of P- and S-wave receiver functions (Vinnik et al., 2009) are consistent with these estimates: the onset of the S wave velocity reduction is found at a depth of 140 ± 20 km. Seismic velocity anomalies at these depths are likely to be associated, at least in part, with melt-metasomatism of the lower portions of the cratonic lithosphere (Artemieva, 2009), as indicated by petrological studies of mantle xenoliths from group I kimberlites (Fig. 11) (O'Reilly and Griffin, 2006). These anomalies down to a ca. 200 km depth are incorporated into the lithosphere mantle density model, and therefore they cannot explain extra 0.5–1.0 km of surface elevation, unexplained by the lithosphere mantle density structure. Note that low-Vs anomalies in the depth range from ca. 200 km down to ca. 250 km depth are below the lithosphere base adopted in the density analysis. If these anomalies are associated with low-density sublithospheric upper mantle material, they may provide the required amplitude of surface elevation. However, for a 50 km thick layer, this would require a significant density reduction (ca. 0.05 g/cm^3, or 1.5%). In case of a thermal origin of such density anomaly, its temperature should be ca. 250–300 deg. higher than ambient mantle (Fig. 10). It is difficult to imagine that the anomaly may have a compositional origin, since it would be gravitationally unstable.

A more likely candidate for mantle dynamic support is the low-velocity layer at depths 300–400 km (perhaps at a 250–400 km depth) (labeled "1" in Fig. 11). A thermal anomaly of 100–200 °C distributed over a 100–150 km thick layer may explain 0.5–1.0 km of extra topographic uplift and it will produce Vs reduction by ca. 2% as reported in seismic studies (Fig. 11, e.g. Wang et al., 2008).

Additionally, seismic studies based on teleseismic S-RF demonstrate the presence of ca. 50 km thick layer with anomalously low S-velocity atop the mantle transition zone beneath South Africa (Vinnik et al., 1996; Vinnik and Farra, 2007) (labeled "2" in Fig. 11). The origin of this anomaly remains enigmatic. In case this low-velocity layer is produced by mantle upwelling across the 410-km discontinuity, it would lead to dehydration of olivine and mantle melting (Bercovici and Karato, 2003). In such a case, seismic data may be explained by the presence of ca. 1 vol% of melt (Hier-Majumder and Courtier, 2011). However, density of the melt is expected to be close to density of dry olivine, and therefore the velocity decrease in the depth interval from 350 km to 410 km may not be accompanied by a density decrease, so that a role of this layer in dynamic topography can be small. However, some contribution of this low-velocity layer to regional topography cannot be fully ruled out, since even a 0.05 g/cm^3 density decrease in a 50 km thick layer may produce the required 0.5 km of surface elevation.

Mantle residual/dynamic topography can also be affected by an increased temperature in the mantle transition zone, such as associated with mantle convective instabilities. The temperature anomaly can be evaluated from the arrival times of seismic Ps converted phases from the 410-km and 660-km discontinuities (P410s and P660s). The Clapeyron slopes of the phase transitions at 410-km and 660-km depths are, respectively, positive and negative (Ito and Takahashi, 1989; Katsura and Ito, 1989). Therefore, a decrease (or an increase) of mantle temperature in the transition zone will, correspondingly, increase (or reduce) its thickness and will increase (or reduce) the related differential time between the arrivals of seismic Ps converted phases from the 410-km and 660-km discontinuities. By a rule of thumb, a reduction of the differential time by 1 s corresponds to the temperature increase of ~100 °C. The anomaly of 1 s can be easily detected by seismic methods, however beneath the Kaapvaal craton the differential time is close to the standard global value of 23.9 s (Vinnik et al., 1996), which makes a significant temperature anomaly in the mantle transition zone unlikely. We therefore conclude that the source of mantle dynamic topography is likely to be located in a 50–150 km thick upper mantle layer below the lithosphere base, which would also explain the regional scale of the high topography in southern Africa.

5. Conclusions

We compare topography in different Precambrian cratons and demonstrate that topography in southern Africa and the Tanzanian region, both in the Archean and Proterozoic blocks, is 500–700 m higher than in any other cratons worldwide.

We present the analysis of mantle dynamic/residual topography (caused by low density mantle anomalies or stresses associated with the mantle flow) and calculate the depth-averaged density structure of the lithospheric mantle in southern Africa. The results demonstrate that contribution of dynamic topography (that is with the origin in the mantle below the lithospheric base) to surface relief in southern Africa is between 0.5 km and 1 km, with the more likely value of ca. 0.5 km.

We propose that the source of regional dynamic topography is related to low-velocity anomaly between the lithospheric base and the mantle transition zone, with the candidate layer being ca. 100–150 km thick and probably associated with a thermal anomaly of 100–200 °C.

We also present the model of the density structure of the lithospheric mantle, further discussed in the companion paper (Artemieva and Vinnik, in review). It shows that lithosphere mantle is laterally highly heterogeneous and density anomalies are well correlated with tectonic provinces and crustal ages.

(i) The Eastern and Western provinces of the Cape Fold Belt have significantly different mantle density structure: low-density mantle of the Western province may include remnants of ancient lithosphere, while high-density mantle of the Eastern province may have include oceanic slabs.

(ii) The lithosphere mantle of the Kaapvaal Craton has low density, except for the Barberton greenstone belt and the Bushveld intrusion, where mantle density is increased to 3.34–3.36 g/cm^3. Similar values are calculated for the Limpopo Belt where the cratonic root may be melt-metasomatised. The mantle of the eastern Zimbabwe Craton has low density and is similar to the Kaapvaal, while the western Zimbabwe has high-density mantle. The discussion of the relationship between the lithosphere mantle density and kimberlite magmatism is in the companion paper (Artemieva and Vinnik, in review).

Supplementary data to this article can be found online at http://dx.doi.org/10.1016/j.gr.2016.03.002.

Acknowledgements

This study is supported by DFF-FNU grant DFF- 1323-00053 to IMA. The IGN-KU grant to IA, which partially supported the long-term research visit by LPV, is gratefully acknowledged. The authors appreciate discussions with Y. Cherepanova at early stages of this study. Our special thanks go to M. Youssof who made his SASE crustal and mantle models available for our modeling. Stimulating discussions with Hans Thybo on the lithosphere structure and gravity anomalies in southern Africa are gratefully acknowledged. The authors are grateful to anonymous reviewer for a number of suggestions which helped us to improve the presentation.

References

Al-Hajri, Y., White, N., Fishwick, S., 2009. Scales of transient convective support beneath Africa. Geology 37, 883–886.

Amante, C., Eakins, B.W., 2009. ETOPO1 1 arc-minute global relief model: procedures, data sources and analysis. NOAA Technical Memorandum NESDIS NGDC-24. National Geophysical Data Center, NOAA http://dx.doi.org/10.7289/V5C8276M.

Artemieva, I.M., 2006. Global 1°×1° thermal model TC1 for the continental lithosphere: implications for lithosphere secular evolution. Tectonophysics 416, 245–277.

Artemieva, I.M., 2007. Dynamic topography of the East European Craton: shedding light upon the lithospheric structure, composition and mantle dynamics. Global and Planetary Change 58, 411–434.

Artemieva, I.M., 2009. The continental lithosphere: reconciling thermal, seismic, and petrologic data. Lithos 109, 23–46.

Artemieva, I.M., Mooney, W.D., 2001. Thermal structure and evolution of Precambrian lithosphere: A global study. Journal of Geophysical Research 106, 16387–16414.

Artemieva, I.M., Vinnik, L.P., 2016. Density structure of the cratonic mantle in southern Africa: 2. Correlations with seismic velocities, kimberlite distribution, and tectonics. Gondwana Research (in review).

Artyushkov, E., Hofmann, A., 1998. Neotectonic crustal uplift on the continents and its possible mechanisms: the case of southern Africa. Surveys in Geophysics 18, 369–415.

Braun, J., 2010. The many surface expressions of mantle dynamics. Nature Geoscience 3, 825–833.

Bercovici, D., Karato, S.-i, 2003. Whole-mantle convection and the transition-zone water filter. Nature 425, 39–44.

Boyd, F.R., Mertzman, S.A., 1987. Composition and structure of the Kaapvaal lithosphere, southern Africa. In: Mysen, B.O. (Ed.), Magmatic Processes: Physiochemical Principles. Geochemical Society, University Park, PA, pp. 13–24.

Brocker, T., 2005. Empirical relations between elastic wavespeeds and density in the Earth's crust. Bulletin of the Seismological Society of America 95, 2081–2092.

Cadek, O., Fleitout, L., 2003. Effect of lateral viscosity variations in the top 300 km on the geoid and dynamic topography. Geophysical Journal International 152, 566–580.

Cammarano, F., Goes, S., Pierre, V., Giardini, D., 2003. Inferring upper-mantle temperatures from seismic velocities. Physics of the Earth and Planetary Interiors 138, 197–222.

Campbell, I.H., Naldrett, A.J., Barnes, S.J., 1983. A model for the origin of the platinum-rich sulfide horizons in the Bushveld and Stillwater complexes. Journal of Petrology 24, 133–165.

Carlson, R.W., Pearson, D.G., Boyd, F.R., Shirey, S.B., Irvine, G.J., Menzies, A.H., Gurney, J.J., Richardson, S.H., 1999. Re–Os systematics of lithospheric peridotites: implications for lithosphere formation and preservation. In: Gurney, J.J., Gurney, J.L., Pascoe, M.D. (Eds.), Proc. 7th Intern. Kimberlite Conf., Cape TownThe J. B. Dawson Volume vol. 1. Red Roof Design, Cape Town, pp. 99–108.

Cherepanova, Y., Artemieva, I.M., 2015. Density heterogeneity of cratonic lithospheric mantle: A case study of the Siberian Craton. Gondwana Research http://dx.doi.org/10.1016/j.gr.2014.10.002.

Conrad, C.P., 2013. The solid Earth's influence on sea level. GSA Bulletin 125, 1027–1052.

Cox, K.G., 1989. The role of mantle plumes in the development of continental drainage patterns. Nature 342, 873–877.

de Wit, M.J., Roering, C., Hart, R.J., Armstrong, R.A., deRonde, C.E.J., Green, R.W.E., Tredoeaux, M., Pederby, E., Hart, R.A., 1992. Formation of an Archaean continent. Nature 357, 553–562.

Doucoure, M.C., de Wit, M., Mushayandebvu, M., 1996. Effective elastic thickness of the continental lithosphere. Journal of Geophysical Research 101, 11,291–11,303.

Downey, N.J., Gurnis, M., 2009. Instantaneous dynamics of the cratonic Congo basin. Journal of Geophysical Research 114 (B6), B06401.

Faure, S., 2006. World kimberlites and lamproites CONSOREM database (version 2006–1). Consortium de Recherché en Exploration Minarale CONSOREM. Université du Quebec á Montreal (Numerical Database, www.consorem.ca).

Flament, N., Gurnis, M., Williams, S., et al., 2014. Topographic asymmetry of the South Africa from global models of mantle flow and lithospheric stretching. Earth and Planetary Science Letters 387, 107–119.

Forte, A.M., Quere, S., Moucha, R., et al., 2010. Joint seismic–geodynamic–mineral physical modelling of African geodynamics: a reconciliation of deep-mantle convection with surface geophysical constraints. Earth and Planetary Science Letters 295, 329–341.

Foulger, G.R., Panza, G.F., Artemieva, I.M., Bastow, I.D., Cammarano, F., Evans, J.R., Hamilton, W.B., Julian, B.R., Lustrino, M., Thybo, H., Yanovskaya, T.B., 2013. Caveats on tomographic images. Terra Nova 25 (4), 259–281.

Gaul, O.F., Griffin, W.L., O'Reilly, S.Y., Pearson, N.J., 2000. Mapping olivine composition in the lithospheric mantle. Earth and Planetary Science Letters 182, 223–235.

Goodwin, A.M., 1996. Principles of Precambrian Geology. Academic Press, London, San Diego, Toronto (327 pp.).

Griffin, W.L., O'Reilly, S.Y., Ryan, C.G., Gaul, O., Ionov, D., 1998a. Secular variation in the composition of continental lithospheric mantle. In: Braun, J., et al. (Eds.), Structure and Evolution of the Australian Continent. AGU Geodynam. Ser 26, pp. 1–25.

Griffin, W.L., O'Reilly, S.Y., Ryan, C.G., 1999b. The composition and origin of subcontinental lithospheric mantle. In: Fei, Y., Bertka, C.M., Mysen, B.O. (Eds.), Mantle Petrology: Field Observations and High Pressure Experimentation: A Tribute to Francis R. (Joe) Boyd. Geochem. Soc. Spec. Publ. No. 6, pp. 13–45.

Griffin, W.L., O'Reilly, S.Y., Natapov, L.M., Ryan, C.G., 2003b. The evolution of lithospheric mantle beneath the Kalahari Craton and its margins. Lithos 71, 215–241.

Griffin, W.L., Natapov, L.M., O'Reilly, S.Y., et al., 2005. The Kharamai kimberlite field, Siberia: modification of the lithospheric mantle by the Siberian Trap event. Lithos 81, 167–187.

Gurnis, M., Mitrovica, J.X., Ritsema, J.S., Van Heijst, H., 2000. Constraining mantle density structure using geological evidence of surface uplift rates: the case of the African super plume. Geochemistry, Geophysics, Geosystems 1, 1020.

Hager, B.H., Clayton, R.W., Richards, M.A., Comer, R.P., Dziewonski, A.M., 1985. Lower mantle heterogeneity; dynamic topography and the geoid. Nature 313, 541–545.

Hanson, R.E., Crowley, J.L., Bowring, S.A., Ramezani, J., Gose, W.A., Dalziel, I.W.D., Pancake, J.A., Seidel, E.K., Blenkinsop, T.G., Mukwakwami, J., 2004. Coeval large scale magmatism in the Kalahari and Laurentian cratons during Rodinia assembly. Science 304, 1126–1129.

Hawkesworth, C.J., Kempton, P.D., Rogers, N.W., Ellam, R.M., van Calsteren, P.W., 1990. Continental mantle lithosphere, and shallow level enrichment process in the Earth's mantle. Earth and Planetary Science Letters 96, 256–268.

Heine, C., Muller, D., Steinberger, B., Torsvik, T., 2008. Subsidence in intracontinental basins due to dynamic topography. Physics of the Earth and Planetary Interiors 171, 252–264.

Herceg, M., Artemieva, I.M., Thybo, H., 2015. Density of the lithospheric mantle beneath the Siberian Craton from GOCE satellite gravity and a new regional crustal model. Journal of Geophysical Research (in submission).

Hier-Majumder, S., Courtier, A., 2011. Seismic signature of small melt fraction atop the transition zone. EPSL 308, 334–342.

IHFC, 2011. International Heat Flow Commission. The global heat flow database. http://www.heatflow.und.edu/index2.html.

Irifune, T., 1987. An experimental investigation of the pyroxene-garnet transformation in a pyrolite composition and its bearing on the composition of the mantle. Physics of the Earth and Planetary Interiors 45, 324–336.

Irvine, G.I., Pearson, D.G., Carlson, R.W., 2001. Lithospheric mantle evolution in the Kaapvaal Craton: a Re–Os isotope study of peridotite xenoliths from Lesotho kimberlites. Geophysical Research Letters 28, 2505–2508.

Ito, E., Takahashi, E., 1989. Postspinel transformation in the system Mg_2 SiO_4–Fe_2SiO_4 and some geophysical implications. Journal of Geophysical Research 94, 10637–10646.

James, D.E., Boyd, F.R., Schutt, D., Bell, D.R., Carlson, R.W., 2004. Xenolith constraints on seismic velocities in the upper mantle beneath southern Africa. Geochemistry, Geophysics, Geosystems 5 (1), Q01002. http://dx.doi.org/10.1029/2003GC000551.

Kashubin, S., Juhlin, C., Friberg, M., et al., 2006. Crustal structure of the Middle Urals based on seismic reflection data. European lithosphere dynamics. In: Gee, D.G., Stephenson, R.A. (Eds.), Geological Society, London, Memoirs 32, pp. 427–442.

Katsura, T., Ito, E., 1989. The system Mg_2SiO_4–Fe_2SiO_4 at high pressures and temperatures: precise determination of stabilities of olivine, modified spinel and spinel. Journal of Geophysical Research 94, 15663–15670.

Kopylova, M.G., Russell, J.K., 2000. Chemical stratification of cratonic lithosphere: constraints from the northern Slave craton, Canada. Earth and Planetary Science Letters 181, 71–87.

Lachenbruch, A.H., Morgan, P., 1990. Continental extension, magmatism and elevation; formal relations and rules of thumb. Tectonophysics 174, 39–62.

Lehtonen, M., O'Brien, H.E., Peltonen, P., Johanson, B.S., Pakkanen, L., 2004. Layered mantle at the Karelian Craton margin: P–T of mantle xenocrysts and xenoliths from the Kaavi–Kuopio kimberlites, Finland. Lithos 77, 593–608.

Li, A., Burke, K., 2006. Upper mantle structure of southern Africa from Rayleigh wave tomography. Journal of Geophysical Research 111 (B10). http://dx.doi.org/10.1029/2006/B004321.

Lithgow-Bertelloni, C., Silver, P.G., 1998. Dynamic topography, plate driving forces and the African superswell. Nature 395, 269–272.

Lowrie, W., 2007. Fundamentals of geophysics. second ed. Cambridge Univ. Press (381 pp.).

McKenzie, D.P., 2010. The influence of dynamically supported topography on estimates of Te. Earth and Planetary Science Letters 295, 127–138.

Mercier, J.-C.C., 1980. Magnitude of the continental lithospheric stresses inferred from rheomorphic petrology. Journal of Geophysical Research 85, 6293–6303.

Molnar, P., England, P., Jones, C.H., 2015. Mantle dynamics, isostasy, and the support of high terrain. Journal of Geophysical Research 120, 1932–1957.

Moucha, R., Forte, A.M., 2011. Changes in African topography driven by mantle convection. Nature Geoscience 4, 707–712. http://dx.doi.org/10.1038/ngeo1235.

Ni, S.D., Helmberger, D.V., 2003. Seismological constraints on the South African superplume; could be the oldest distinct structure on Earth. Earth and Planetary Science Letters 206, 119–131.

Nyblade, A.A., Robinson, S.W., 1994. The African superswell. Geophysical Research Letters 21, 765–768.

O'Reilly, S.Y., Griffin, W.L., 2006. Imaging global chemical and thermal heterogeneity in the subcontinental lithospheric mantle with garnets and xenoliths: geophysical implications. Tectonophysics 416, 289–309.

Pavlis, N.K., Holmes, S.A., Kenyon, S.C., Factor, J.K., 2012. The development and evaluation of the earth gravitational model 2008 (EGM2008). Journal of Geophysical Research 117 (B4).

Pearson, D.G., Wittig, N., 2008. Formation of Archaean continental lithosphere and its diamonds: the root of the problem. Journal of the Geological Society 165, 895–914.

Priestley, K., McKenzie, D., Debayle, E., 2006. The state of the upper mantle beneath southern Africa. Tectonophysics 416 (1–4), 101–112.

Riley, T.R., Curtis, M.L., Leat, P.T., et al., 2006. Overlap of Karoo and Ferrar magma types in KwaZulu-Natal, South Africa. Journal of Petrology 47, 541–566.

Ritsema, J., Van Heijst, H., Woodhouse, J., 1999. Complex shear wave velocity structure related to mantle upwellings beneath Africa and Iceland. Science 286, 1925–1928.

Rozendaal, A., Gresse, P.G., Scheepers, R., Le Roux, J.P., 1999. Neoproterozoic to early Cambrian crustal evolution of the Pan-African Saldania Belt, South Africa. Precambrian Research 97, 303–323.

Rudnick, L.R., Nyblade, A.A., 1999. The thickness and heat production of Archean lithosphere: constraints from xenolith thermobarometry and surface heat flow. In: Fei, Y., Bertka, C.M., Mysen, B.O. (Eds.), Mantle Petrology: Field Observations and High Pressure Experimentation: A Tribute to Francis R. (Joe) Boyd. Chem. Soc. Spec. Publ. No. 6, pp. 3–12.

Schmitz, M.D., Bowring, S.A., 2003. Ultrahigh-temperature metamorphism in the lower crust during Neoarchean Ventersdorp rifting and magmatism, Kaapvaal Craton, southern Africa. Geological Society of America Bulletin 115, 533–548.

Simmons, N.A., Forte, A.M., Grand, S.P., 2007. Thermochemical structure and dynamics of the African super-plume. Geophysical Research Letters 34, L02301.
Simon, N.S.C., Carlson, R.W., Pearson, D.G., Davies, G.R., 2007. The origin and evolution of the Kaapvaal cratonic lithospheric mantle. Journal of Petrology 48, 589–625.
Smith, C.B., Pearson, D.G., Bulanova, G.P., et al., 2009. Extremely depleted lithospheric mantle and diamonds beneath the southern Zimbabwe Craton. Lithos 112, 1120–1132.
Thybo, H., Artemieva, I.M., 2013. Moho and magmatic underplating in continental lithosphere. Tectonophysics 609, 605–619.
Vinnik, L., Farra, V., 2007. Low S velocity atop the 410-km discontinuity and mantle plumes. Earth and Planetary Science Letters 262 (3–4), 398–412.
Vinnik, L.P., Green, R.W.E., Nicolaysen, L.O., Kosarev, G.L., Petersen, N.V., 1996. Deep seismic structure of the Kaapvaal craton. Tectonophysics 262 (1–4), 67–75.
Vinnik, L., Oreshin, S., Kosarev, G., Kiselev, S., Makeyeva, L., 2009. Mantle anomalies beneath southern Africa: evidence from seismic S and P receiver functions. Geophysical Journal International 179 (1), 279–298.
Vinnik, L., Kiselev, S., Weber, M., Oreshin, S., Makeyeva, L., 2012. Frozen and active seismic anisotropy beneath southern Africa. Geophysical Research Letters 39, L08301. http://dx.doi.org/10.1029/2012GL051326.
Wang, Yi, Wen, L., Weidner, D., 2008. Upper mantle SH- and P-velocity structures and compositional models beneath southern Africa. Earth and Planetary Science Letters 267, 596–608.
Youssof, M., Thybo, H., Artemieva, I.M., Levander, A., 2013. Moho depth and crustal composition in southern Africa. Tectonophysics 609, 267–287.